Viscoelastic properties of semiflexible filamentous bacteriophage fd

Frank G. Schmidt,[1] Bernhard Hinner,[1] Erich Sackmann,[1] and Jay X. Tang,[2,*]
[1]*Technische Universität München, Institut für Biophysik E22, James-Franck- Strasse, D-85747 München, Germany*
[2]*Department of Physics, Indiana University, 727 East Third Street, Bloomington, Indiana 47405*
(Received 6 January 2000)

The cytoskeletal protein filament *F*-actin has been treated in a number of recent studies as a model physical system for semiflexible filaments. In this work, we studied the viscoelastic properties of entangled solutions of the filamentous bacteriophage fd as an alternative to *F*-actin with similar physical parameters. We present both microrheometric and macrorheometric measurements of the viscoelastic storage and loss moduli, $G'(f)$ and $G''(f)$, respectively, in a frequency range $0.01<f<4$ Hz, for fd solutions in the concentration range $5<c<15$ mg/ml. The onset of a narrow and slanted plateaulike region of $G'(f)$ is located at around 2 Hz. The variation of the plateau modulus with concentration obeys a power law $G'_N \propto c^{1.4\pm0.3}$, similar to that found for entangled solutions of *F*-actin. In the low-frequency regime, the frequency dependence of the viscoelastic moduli can be described by power laws $G'(f)\propto f^{0.9-1.2}$ and $G''(f)\propto f^{0.7-0.9}$, which deviate significantly from the simple theoretical predictions of $G'(f)\propto f^2$ and $G''(f)\propto f^1$. The latter behavior cannot yet be understood within the framework of current theories of semiflexible filament networks. For the dynamic viscosity at the low shear rate limit, a concentration dependence of $\eta_0 \propto c^{2.6}$ was found. Finally, a linear scaling of the terminal relaxation time with concentration, $\tau_d \propto c$, was observed.

PACS number(s): 87.15.−v, 83.10.Nn, 83.50.Fc, 83.80.Lz

I. INTRODUCTION

Rheological properties of networks of sterically interacting semiflexible filaments are a subject of great current interest and of intense experimental and theoretical studies. One motivation of such studies is that a number of biological polymers such as the cytoskeletal proteins *F*-actin and intermediate filaments, as well as polyelectrolytes, belong to this class of polymers. In addition, the structural and mechanical properties of networks formed by semiflexible macromolecular filaments are determined by entropic and enthalpic contributions. This is in contrast to flexible polymers, the properties of which are determined exclusively by entropic effects. The rheological properties of semiflexible polymers are therefore not well described by traditional theories for flexible polymers [1,2]. Recent theoretical efforts have emerged to provide a conceptual foundation for networks of semiflexible filaments [3–18].

Much of the recent theoretical development has been aimed at predicting the rheological behavior of *F*-actin networks [6,8–11,15]. This is because most experimental studies of a semiflexible filament network are based on solutions of *F*-actin as a model polymer. However, among a large number of reports from several laboratories, the values of viscoelastic storage and loss moduli, $G'(f)$ and $G''(f)$, respectively, differ by as much as three orders of magnitude [19,20]. This large variance is due to the fact that the rheologic properties of *F*-actin solutions are extremely sensitive to the presence of even small traces of cross-linkers (cf., e.g., [20–22]) or capping proteins (cf., e.g., [23]), which modify *F*-actin networks in living cells [24]. It has been shown more recently that cross-linking can also occur due to a slow oxidation of actin, which produces a small percentage of disulfide-bonded actin dimers that are capable of cross-linking actin filaments during polymerization [25]. The large variance of filament length between preparations from different laboratories, as well as polydispersity that is exhibited by the filaments in *F*-actin solutions, further compounds attempts to provide a coherent set of data. The average filament length can be regulated and adjusted by the use of capping proteins mentioned above, but the solutions will remain polydisperse. These practical problems seriously interfere with reliable comparisons between theory and experiment. One practical solution is to find an alternative species of semiflexible filaments with similar length and persistence length as *F*-actin, and to check the theoretical predictions with such a system.

The filamentous bacteriophage fd fulfills this role. It is a semiflexible filament with a uniform length of $L_{\rm fd}=0.9\,\mu$m [26,27], a persistence length of $L_p=2.2\,\mu$m [28–30], and a molecular mass $M_{\rm fd}=16.4\times10^6$ Da. The diameter of fd ($d_{\rm fd}=7$ nm) and its linear mass density ($\sigma_{\rm fd}=18\,200$ kDa/μm) are comparable to an actin filament ($d_{\rm actin}=8$ nm, $\sigma_{\rm actin}=15\,400$ kDa/μm). The aspect ratio, $\epsilon=L/d$, of fd ($\epsilon_{\rm fd}=130$) is comparable to *F*-actin with an average filament length of $L=1.5\,\mu$m ($\epsilon_{\rm actin}=190$). Solutions of fd have been used extensively as a model system in studies of particle dynamics by dynamic light scattering [28–31], formation of liquid-crystalline phases [32–34], and the polyelectrolyte behavior of highly charged filamentous biopolymers [35,36]. In the present work we measured the viscoelastic impedance spectra of entangled networks of fd solutions by torsional rheometry and magnetic bead microrheometry in the frequency range $f=0.01-4$ Hz. The results are compared with the frequency dependence of the storage and loss modulus of entangled *F*-actin solutions of similar filament length, and with theoretical predictions.

*Author to whom correspondence should be addressed. Fax: 812 855 5533. Email address: jxtang@indiana.edu

II. MATERIALS AND METHODS

A. Preparation of bacteriophages

The fd phage was prepared by a standard method [37]. The virus suspensions were kept in a buffer solution containing 3 mM Tris-Cl at a pH 8.0, 100 mM NaCl, and 1 mM NaN_3. The virus particles are stable in solution at 4 °C over a period of several months.

B. Electron microscopy

The negative staining technique was used to visualize fd filaments by electron microscopy (EM). Briefly, the EM grids were coated with formvar films, followed by carbon coating and treatment of glow discharge. A 10-μl drop of approximately 0.1 mg/ml fd solution was deposited onto an EM grid that had been rinsed with several drops of distilled water. After adsorption for 1 min, the aqueous solution was removed with filter paper, and the sample was negatively stained with 0.8% uranyl acetate for 1 min. Excess liquid was again drained with filter paper. The sample was then examined at 100 kV using a Philips CM 100 electron microscope. Pictures were taken using Agfa Scientia electron image films.

C. Rheometry

Three instruments were used to obtain the viscoelastic properties of fd networks. One of the three instruments, previously described as a magnetic tweezers rheometer [38], enables one to measure local viscoelastic properties on a scale of a few micrometers, therefore it is a ''microrheometric'' method. The other two rheometers measure macroscopic bulk properties, which will be referred to as ''macrorheometric'' measurements as described below.

1. Magnetic tweezers rheometry

The physical principle and instrumental details of a home-built magnetic tweezers rheometer have been described previously [38–40]. Briefly, spherical superparamagnetic beads with a diameter of $2R=4.5\,\mu$m (Dynabeads M-450, Deutsche Dynal, Hamburg) are embedded within the network. The beads are manipulated by an external magnetic field (hence the name magnetic tweezers). The motions of single beads induced by oscillatory magnetic fields are monitored by particle tracking using videomicroscopy and image processing. The magnetic force is controlled by the voltage signal generated by a function generator. By applying a sinusoidal force of frequency f and by recording the oscillatory voltage signal simultaneously with the induced displacements of the beads, the viscoelastic storage and loss moduli $G'(f)$ and $G''(f)$, respectively, can be determined following a previously described procedure [40]. The magnetic tweezers rheometer is well suited for measurements of very soft materials, with an applicable frequency range from below 10 mHz up to 5 Hz.

2. Macroscopic rheometry

Independent sets of measurements were performed using a magnetically driven rotating-disk rheometer, as described previously [41,42]. At the upper bound frequency above 3 Hz, the results from the instrument are no longer reliable in the case of the fd solutions used, since the results are influenced by the inertia of the instrument. For this reason, results obtained with this instrument are only shown for frequencies $f<3$ Hz.

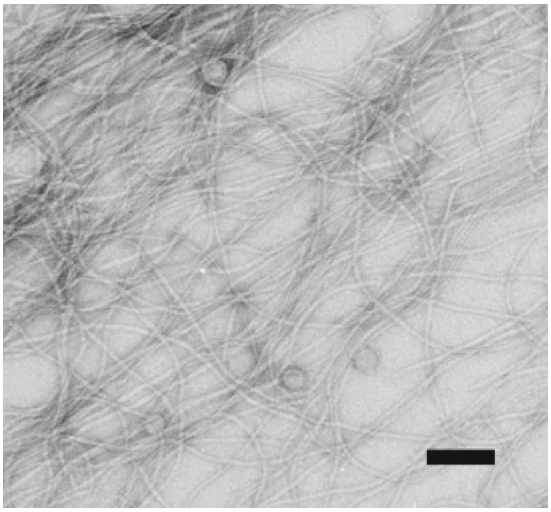

FIG. 1. Negative staining electron micrograph of an fd virus network. The scale bar at the lower right represents 100 nm.

A commercial macroscopic rheometer such as a Rheometrics RFS II (Rheometrics Scientific, Piscataway, NJ) can measure shear moduli as functions of frequency up to about 15 Hz, higher than the practical limit of the home-built magnetically driven rotating-disk rheometer. A severe limitation of such a commercial instrument, however, is its practical sensitivity limit of 10^{-10} N m torque, using a cone-and-plate pair with a diameter of 50 mm. In this work, since the network strength of fd is very weak, a Rheometrics RFS II rheometer was used only for selected rheological measurements of high fd concentrations of 10 mg/ml or above.

III. RESULTS

With a persistence length of 2.2 μm and a length of 0.9 μm, fd viruses are best described as semiflexible filaments. Judged from the electron micrographs prepared by the negative staining technique, the dispersion of filaments forms an interconnected network (Fig. 1). Observations based on both EM and separate light-scattering studies [50] confirm that the fd filaments do not aggregate, which is an important requirement for the comparison of our experimental results with theoretical predictions.

Measurements of storage and loss moduli, $G'(f)$ and $G''(f)$, respectively, have been carried out in the frequency range $f=0.01-4$ Hz using fd solutions of concentrations $c_{\mathrm{fd}}=5-15$ mg/ml. The results of a few representative measurements are shown in Fig. 2. The loss modulus is larger than the storage modulus, $G''(f)>G'(f)$, for all frequencies below 1 Hz. At frequencies above 1 Hz, a shallow plateaulike region with $G'(f)\approx G''(f)$ is observed based on the microrheometric data. The loss modulus, $G''(f)$, exhibits an inflection point around $f\approx 1$ Hz. Plots of the loss tangent, $G''(f)/G'(f)$, suggest that its value is nearly constant at $f\approx 2$ Hz, except for the two low concentrations in which cases the data are less reliable (see the scatter on the lower right graph of Fig. 2). At lower frequencies of $f<1$ Hz,

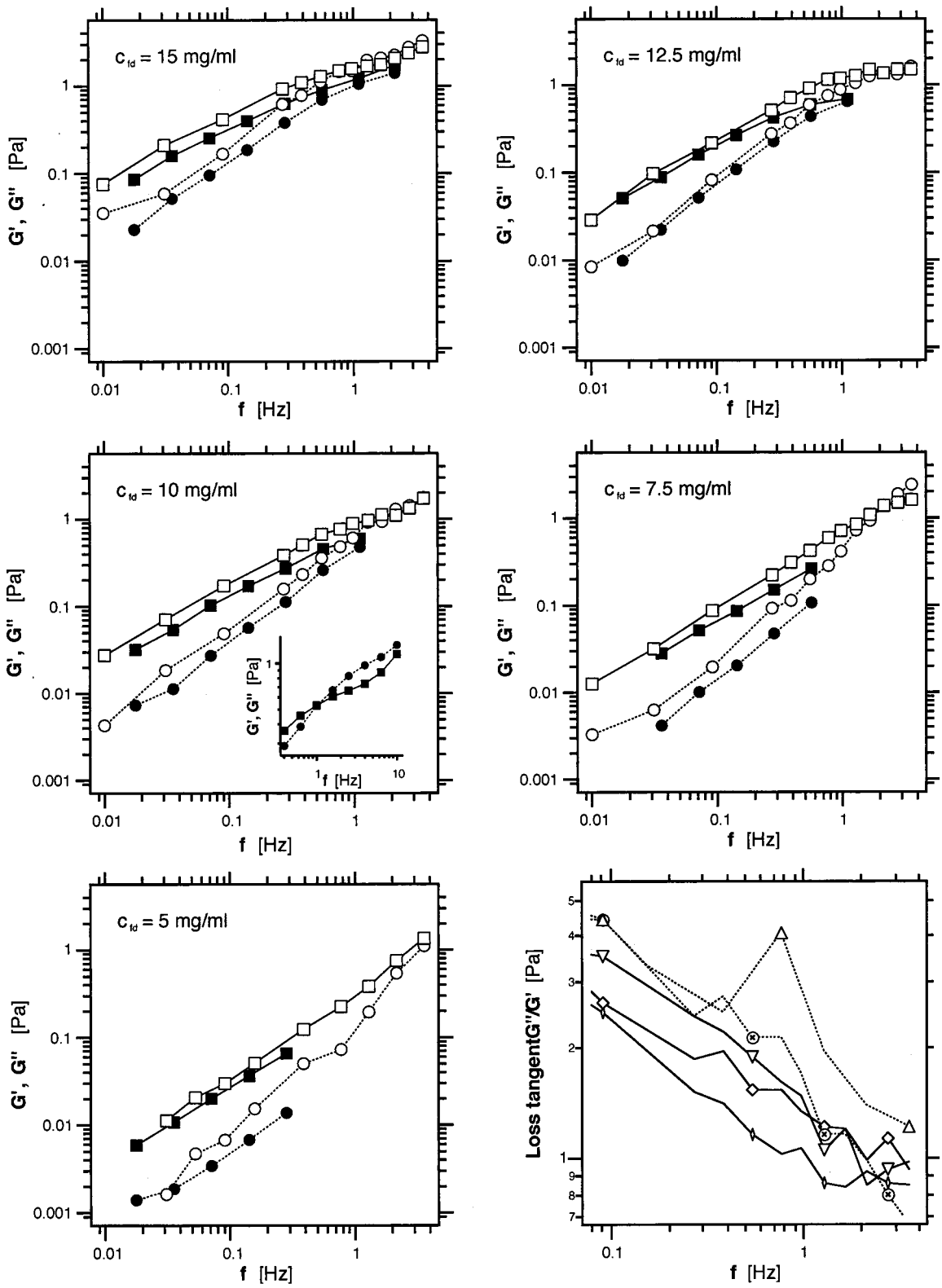

FIG. 2. Results from microrheological (open symbols) and macroscopic (filled symbols) measurements of $G'(f)$ (circles) and $G''(f)$ (squares) as a function of frequency for solutions of fd viruses of concentrations $c_{\mathrm{fd}}=15$ mg/ml (upper left), 12.5 mg/ml (upper right), 10 mg/ml (middle left), 7.5 mg/ml (middle right), and 5 mg/ml (lower left). All macroscopic results were obtained by rotating-disk rheometry except for the data presented in the inset of $c_{\mathrm{fd}}=10$ mg/ml, which were measured by a commercial RFS II rheometer (see Sec. II). Lower right: Loss tangent, $G''(f)/G'(f)$, in the frequency range of 0.1–4 Hz as calculated from microrheometry. $\diamond$; 15 mg/ml; $\square$, 12.5 mg/ml; $\triangledown$, 10 mg/ml; $\otimes$, 7.5 mg/ml; $\triangle$ 5 mg/ml. A constant value of $G''(f)/G'(f)$ around 2 Hz can be seen at higher concentrations (solid lines). The data become unreliable at lower concentrations (dotted lines).

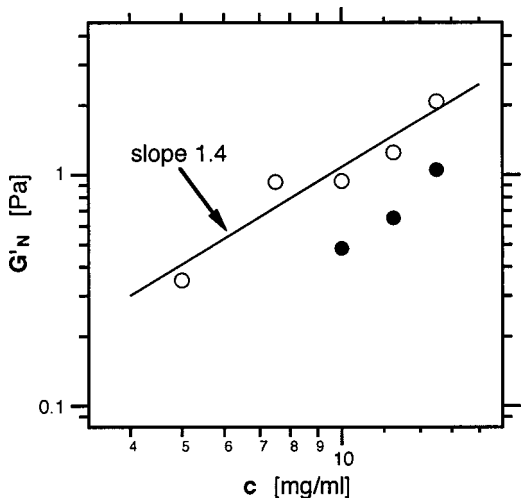

FIG. 3. Plateau modulus, G_N', of fd virus solutions as a function of concentration. Plot of storage modulus at frequency $f=1.7$ Hz from microrheological measurements (○) and at $f=1.1$ Hz from macroscopic measurements (●). The straight line is a power-law fit to the microrheological results of the identified plateau values.

$G''(f)/G'(f)$ decreases with increasing frequency. Our data for the fd samples are similar to the results obtained for entangled actin solutions with an average filament length of 1.5 μm [6]. For the case of *F*-actin one observes the onset of a plateaulike region in the G' versus f plot at about 0.2 Hz, and an inflection point in the G'' versus f plot in the same region. In order to compare the fd results with those found for actin networks, we attribute the flat region of $G'(f)$ at 2 Hz to a plateau.

The concentration dependence of the plateau modulus, $G_N'(c_{\mathrm{fd}})$, was examined by considering the value of $G'(f)$ at the fixed frequency $f=1.7$ Hz. This frequency lies within the plateaulike region for most concentrations (except for $c_{\mathrm{fd}}=5$ mg/ml). Around this frequency, an inflection point was observed in the G'' versus f plot. Therefore, the corresponding value of $G'(f)$ is assumed as the plateau modulus, G_N', of the actin solution (cf. [6]). This is an approximation, since the exact position of the inflection point cannot be located precisely based on the measured data. The result is shown in Fig. 3. It is interesting to note that the frequency at which the plateau is found does not vary markedly with concentration for $c_{\mathrm{fd}} \geqslant 7.5$ mg/ml.

A simple power-law fit, $G_N'(c) \propto c^{\alpha}$, to the data of Fig. 3 in the concentration range of 5–15 mg/ml results in a power $\alpha=1.4\pm0.3$ (drawn line in Fig. 3). We obtain the same power law, if the mean value of $G'(f)$ in the range $f=1.3$–2.2 Hz is plotted against concentration (data not shown). Thus the data from microrheometric measurements of fd phages agree well with a scaling behavior of the plateau modulus $G_N' \propto c_{\mathrm{fd}}^{1.4}$, previously observed for entangled *F*-actin solutions [6,43]. This behavior was also predicted by recent theoretical analysis [6,8,15].

The macroscopic measurements with the rotating-disk rheometer yield reliable results for $c_{\mathrm{fd}}=10$–15 mg/ml at frequencies up to 1.1 Hz, while the data severely scatter above this limit (not shown). Values of $G'(f=1.1\,\mathrm{Hz})$ obtained by macroscopic measurements are also plotted in Fig. 3. These results suggest the same scaling behavior for $G_N'(c_{\mathrm{fd}})$ as microrheometry. There is no significant discrepancy between the macroscopic and microscopic values for G_N', as displayed in Fig. 3, since G' has been evaluated at different frequencies. The relation between microrheology and macrorheology for *F*-actin solutions has been studied and discussed elsewhere [39].

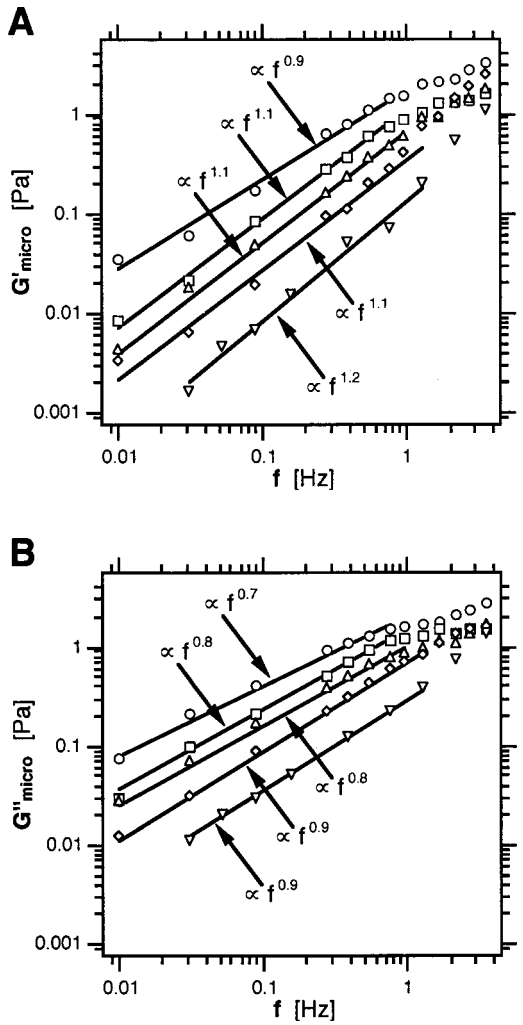

FIG. 4. Power-law behavior of $G'(f)$ (a) and $G''(f)$ (b) at the low-frequency regime. The data from the microrheological measurements of Fig. 2 are shown. The straight lines represent best fits of scaling laws in the respective frequency range for the following five concentrations: 15 mg/ml (○), 12.5 mg/ml (□), 10 mg/ml (△), 7.5 mg/ml (◇), and 5 mg/ml (▽).

The fd solutions exhibit liquidlike features in the frequency range below the plateau region ($f<1$ Hz), and this behavior extends over most of the observed frequency range. In the following, we explore the frequency dependence of the viscoelastic moduli by considering only the data obtained by microrheological measurements, since microrheological and macrorheological results agree quite well but the microrheometric data extend over a broader range of frequencies. The results for several concentrations are summarized in Fig. 4. By analyzing the results in terms of scaling laws, we find empirically $G'(f) \propto f^{0.9-1.2}$ and $G''(f) \propto f^{0.7-0.9}$, respectively. The exponent for $G'(f)$ increases slightly with decreasing concentrations, while for $G''(f)$, the variation is smaller and falls within the experimental uncertainty.

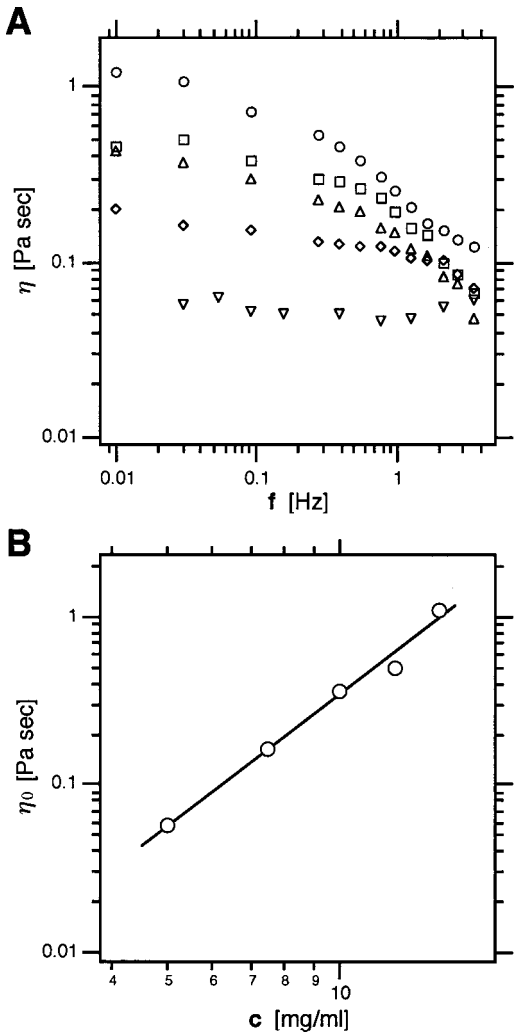

FIG. 5. Frequency and concentration dependence of the dynamic viscosity of fd solutions. (a) Dynamic viscosity as a function of frequency for fd concentrations of 15 mg/ml (○); 12.5 mg/ml (□); 10 mg/ml (△); 7.5 mg/ml (◇); and 5 mg/ml (▽). All values are calculated based on the G'' data of Fig. 2. (b) Concentration dependence of zero-shear viscosity, η_0, estimated from the low-frequency saturation behavior of the dynamic shear viscosity, as described in the text. The value of $\eta(f)$ at $f=0.03$ Hz is used as a measure for η_0. The line fit corresponds to a slope of 2.6.

The dynamic shear viscosity of the fd virus solutions can be calculated from $G''(f)$ by using the relation $\eta(f)=G''(f)/2\pi f$. The results of this analysis are shown in Fig. 5(a). Since the value of $\eta(f)$ is approximately constant at $f\leqslant 0.03$ Hz, the value η (0.03 Hz) is taken as a good approximation of the zero-shear viscosity $\eta_0=\lim_{f\to 0}\eta(t)$. The values thus obtained are shown as a function of fd concentration in Fig. 5(b). Note that at 0.03 Hz the value of $\eta(f)$ is not exactly constant, especially for the solutions with higher c_{fd}. As a consequence, the real value of the zero-shear viscosity is not yet reached. A simple fit to this low shear viscosity data suggests that the dependence of η_0 on concentration can be described by a power law $\eta_0\propto c_{\mathrm{fd}}^{2.6}$ [Fig. 5(b)]. For rigid rods one expects $\eta_0\propto c^3$ [44].

Finally, the terminal relaxation time, τ_d, was obtained using the condition $G'(1/\tau_d)=G'_N/2$ [6]. A linear scaling with concentration, $\tau_d\propto c$, was found (Fig. 6), while for rigid rods $\tau_d\propto c^2$ is expected [44].

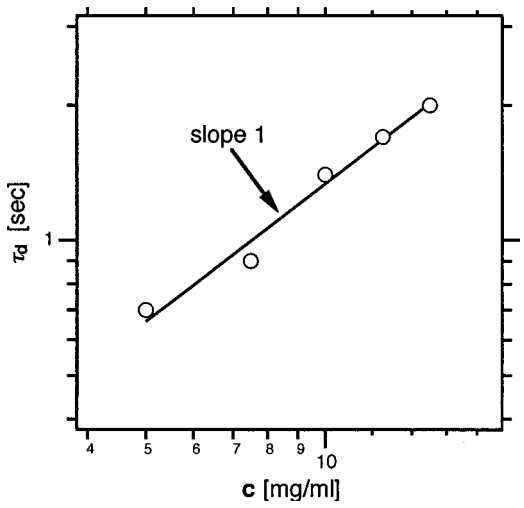

FIG. 6. Concentration dependence of terminal relaxation time of fd virus solution. A power-law fit gives rise to a scaling exponent of 1, shown as a straight line through the data.

IV. DISCUSSION

We studied the viscoelastic properties of solutions of the filamentous bacteriophage fd, which is an excellent model of entangled networks of monodisperse semiflexible filaments. The viscoelastic moduli were measured by macroscopic and microscopic rheometry over a frequency range of $f=0.001-4$ Hz and for concentrations varying from 5 to 15 mg/ml corresponding to volume fractions of $\phi_{\mathrm{fd}}=6.4\times10^{-3}$ to 2×10^{-2}. At these volume fractions, fd forms isotropic networks under the ionic conditions used in our experiments, and the spontaneous formation of a liquid crystalline phase does not occur at concentrations below 20 mg/ml [34].

We shall discuss our findings in the context of recently developed theoretical concepts for rheology of entangled semiflexible polymer solutions. In particular, we will compare the rheologic properties of fd to those found for *F*-actin of similar filament length, such as $L_{\mathrm{actin}}=1.5\,\mu$m [6]. The concentration range of these *F*-actin solutions was from $c_{\mathrm{actin}}=1.35-4.5$ mg/ml, which corresponds to volume fractions from $\phi_{\mathrm{actin}}=2\times10^{-3}$ to 6.7×10^{-3}. In all cases the *F*-actin solutions were isotropic as well. The mesh size of an fd network is defined similarly to that of *F*-actin using the empirical relationship

$$\xi_m=\xi_0\left(\frac{c}{1\ \mathrm{mg/ml}}\right)^{1/2}$$

(Ref. [45]). The numerical coefficient ξ_0 was experimentally determined to be 0.35 μm for pure actin solutions [45]. We adopt $\xi_0=0.6\,\mu$m in the discussion here, which gives rise to the best agreement between theoretical predictions and experimental values of the plateau modulus G'_N for 1.5-μm actin solutions [6] and also for fd solutions, as will be shown below. The mesh size ranged for actin from 0.24 to 0.43 μm, and for fd from 0.16 to 0.26 μm. In order to estimate the entanglement length L_e and the tube diameter d_e, respectively, we apply the simple scaling relationship L_e

$\propto L_p(cLL_p^2)^{-2/5}$ and $d_e \propto L_p(cLL_p^2)^{-3/5}$ [17]. By taking $L = 0.9\,\mu$m as the filament length and $L_p = 2.2\,\mu$m as the persistence length of fd, one obtains $L_e = 115$ nm and $d_e = 26$ nm in a 10 mg/ml fd solution. Thus by using the above scaling relations, a 10 mg/ml fd solution is highly entangled and the tube model predicts on average eight collisions per filament. The small tube diameter and the relatively large collision number approximately satisfy the criteria of recent theoretical models [6,8,15] despite the short filament length of only 0.9 μm.

As it has been pointed out in more detail in Sec. III, a slanted and narrow plateau or a plateaulike region is found in the frequency range $f \geqslant 2$ Hz (Fig. 2). For 1.5 μm *F*-actin a similar region was found around 0.2 Hz [6]. This shift in frequency is due to the larger average filament length of the actin samples. The values of G_N' range for fd from 0.35 to 2.1 Pa and for 1.5 μm *F*-actin from 0.10 to 0.43 Pa. This difference reflects the higher concentrations and smaller persistence length of the fd virus. One important possibility to test theoretical predictions against experimental data is to consider the variation of the plateau modulus, G_N', with concentration. A scaling law of $G_N' \propto c_A^{7/5}$ is expected on the basis of theoretical predictions for semiflexible polymers [6,8,15]. Recent experimental studies of the case of *F*-actin confirm this prediction [6,43]. The same behavior is found for solutions of fd, if one considers the whole range of concentration of $5 \leqslant c_{\mathrm{fd}} \leqslant 15$ mg/ml (cf. the drawn line in Fig. 3).

We now compare recent theoretical predictions with our experimental results concerning the storage modulus in the plateaulike region. A series of recent papers by Morse predict the viscoelastic behavior of a semiflexible polymer network based on a detailed calculation of a stress tensor [13–15], considering local forces and torques. The response to an oscillatory deformation of a semiflexible filament network may be separated into several terms, which have distinct and well separated values and decay times. First, a rapid distortion of the network will result at short time scales in the stretching or compression of the randomly curved filaments, which gives rise to a large tensional stress. The tensional stress has been previously analyzed in detail by MacKintosh *et al.* [10]. Second, the subsequent shear deformation of the network (which is a much slower process) causes bending of the filaments, which leads to a curvature stress. Certain features of the curvature stress have also been predicted by other treatments, such as its dependence on concentration to be $c^{7/5}$ [6,8,11]. Third, the deformation causes changes in filament orientation, thus giving rise to an orientational stress. The orientational stress is negligibly small for long and flexible polymers ($L \gg L_p$), while for suspensions of rigid rods it is the only stress term [44].

Morse's theoretical estimate of the storage modulus can be compared to our values for the plateau modulus, G_N', by assuming that the curvature stress is the dominant term. Taking the 10 mg/ml fd sample for example, a simple estimate of the curvature stress using $G_{\mathrm{curve}} \approx (nL/L_e)k_BT$ (where n denotes the number density of filaments, k_B the Boltzmann constant, and T the absolute temperature) [13] gives a value of 12 Pa. This estimated value is a few times higher than the measured value at the high-frequency limit of 4 Hz, which could be due to neglecting a numerical prefactor in the theoretical estimate, or to the fact that the experimental frequency has not reached the plateau region.

The theoretical approach of Hinner *et al.* [6] leads to a prediction of absolute values of G_N'. The interaction of the polymers with each other is described by means of the tube concept, developed by Odijk [46] and Semenov [17] for semiflexible polymers. Modes of wavelengths smaller than the entanglement length L_e are already equilibrated on the time scale of the plateau regime. Consequently, the viscoelastic response of entangled solutions is dominated by the steric interaction between the tubes, confining the motion of each polymer chain. The plateau modulus of a solution of such tubes can be expressed in terms of a virial expansion. This approach is similar to that accepted to determine the osmotic pressure of dispersed rods [47], except that it is applied to tubes instead of filaments. With this concept, one obtains $G_N' = \frac{9}{5}(k_BT/\xi_m^2 L_e)$ and $L_e \approx 0.58\xi_m^{4/5}L_p^{4/5}$. Applying this equation while taking a numerical coefficient of $\xi_0 = 0.6\,\mu$m for the estimation of the mesh size, i.e.,

$$\xi_m = 0.6\,\mu\mathrm{m} \times \left(\frac{c}{1\ \mathrm{mg/ml}}\right)^{1/2},$$

one finds a remarkably good agreement between theory and experiment: the theoretical curve coincides with the drawn line in Fig. 3.

Now we shall compare the dynamic properties of the entangled fd virus and *F*-actin solutions. The estimated values of the zero shear viscosity of the fd samples range from 5.8×10^{-2} to 1.1 Pa s. For 1.5 μm *F*-actin it was not possible to extrapolate to the limiting frequency, $f \to 0$, since no saturation of the viscosity occurred within the accessible frequency range [51]. In the latter case the viscosity at the smallest frequency, $f = 2 \times 10^{-4}$ Hz, ranges from 2.7 to 9.4 Pa s. For the concentration dependence of the approximate zero-shear viscosity of the fd solution, we find a scaling law $\eta_0 \propto c^{2.6}$ [Fig. 5(b)]. This result can be well understood in terms of a modified Doi model. In its original form, this model predicts a scaling law $\eta_0 \propto c^3$ for solutions of rigid rods in the semidilute and concentrated regime [44]. It is possible to extend this model to treat semiflexible filaments in the following way [48]: η_0 is related to G_N' and the terminal relaxation time, τ_d, by the relation

$$\eta_0 \approx G_N' \tau_d, \tag{4.1}$$

where τ_d scales with the reciprocal coefficient of rotational diffusion, D_r, as

$$\tau_d = \frac{1}{6D_r}. \tag{4.2}$$

For the semidilute to concentrated regime, D_r can be obtained from the rotational diffusion coefficient for dilute solutions, D_{r0}, by using the relation [44]

$$D_r \propto D_{r0}(d/L)^2, \tag{4.3}$$

where d denotes the tube diameter and L the contour length of the filaments. The dependence of D_r on the factor $(d/L)^2$ holds for rigid rods as well as for semiflexible filaments. For the semiflexible case, d obeys the scaling relation [17]

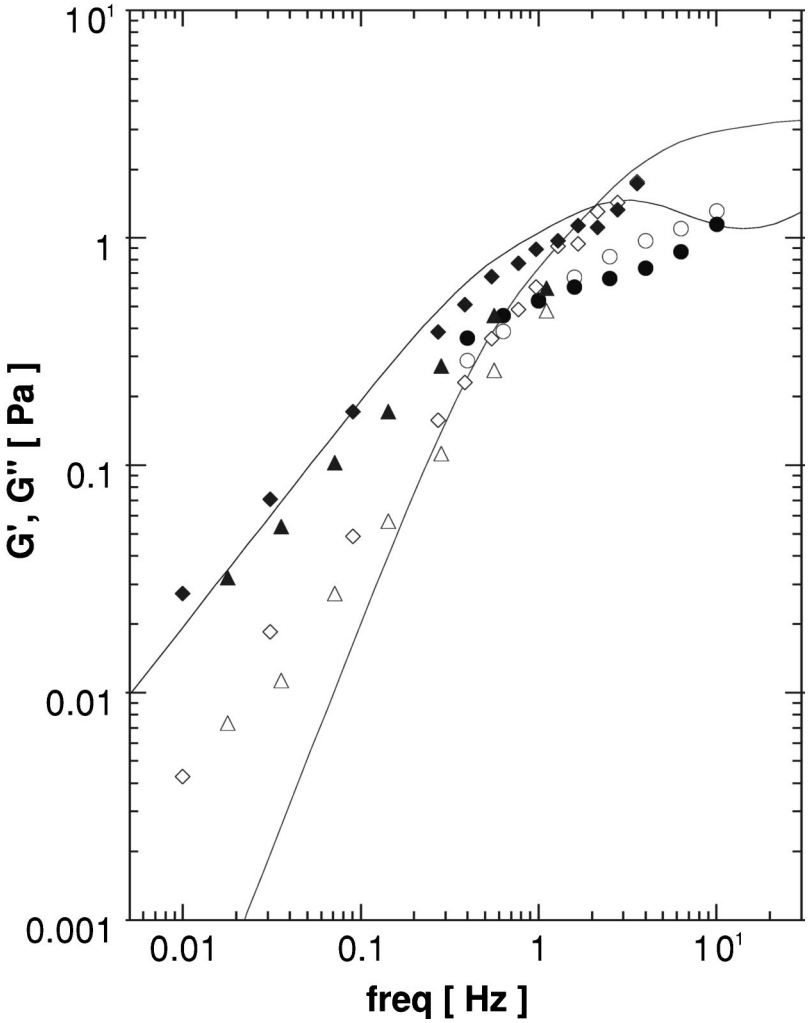

FIG. 7. Comparison between measured shear moduli for a concentration of 10 mg/ml with theoretical predictions based on the analysis of Morse [13]. Solid and hollow symbols represent G' and G'', respectively. Circles, triangles, and diamonds indicate measurements by the RFS II, rotating disk, and magnetic beads rheometry, respectively.

$$d \propto c^{-3/5} L_p^{-1/5}, \tag{4.4}$$

whereas for rigid rods $d \propto c^{-1} L^{-2}$ [44]. Combining Eqs. (4.2)–(4.4) yields the terminal relaxation time of semiflexible filaments,

$$\tau_d \propto c^{6/5}, \tag{4.5}$$

while $\tau_d \propto c^2$ holds for rigid rods [44]. Furthermore, for semiflexible filaments the plateau modulus depends on concentration as [6,8,11]

$$G'_N \propto c^{7/5}, \tag{4.6}$$

whereas $G'_N \propto c$ for rigid rods [44]. Inserting Eqs. (4.5) and (4.6) into Eq. (4.1) yields, finally,

$$\eta_0 \propto c^{13/5} \tag{4.7}$$

for the zero-shear viscosity of solutions of semiflexible filaments. The scaling relation (4.7) is in excellent agreement with our experimental finding of $\eta_0 \propto c_{\mathrm{fd}}^{2.6}$. Furthermore, if all numerical prefactors are retained through the above derivation, one obtains

$$\eta_0 = 9.4 \times 10^{-3}\ \mathrm{Pa\ s} \times \left(\frac{c}{1\ \mathrm{mg/ml}} \right)^{13/5}.$$

This numerical coefficient results in values higher than the experimental data by a factor of about 10. This discrepancy suggests here that the dynamics of semiflexible polymers is still poorly understood, while the static properties, such as the plateau modulus, are already well described by the existing theories.

The values of the terminal relaxation time, τ_d, of the fd solutions range from 0.7 to 2 s. Figure 6 shows that τ_d scales linearly with concentration. As derived above [cf. Eq. (4.5)], an exponent of 6/5 is expected for semiflexible polymers as opposed to 2 for rigid rods. Comparison of the experimental and the theoretical values shows that theory and experiment differ by a factor of 10. This means that the reptation tubes decay faster than theoretically predicted. For *F*-actin filaments of 1.5-μm contour length, one obtains values of τ_d between 25 and 55 s, which do not systematically depend on concentration [50].

In conclusion it is possible to compare the static scaling laws of the plateau modulus of the fd virus and *F*-actin, whereas the scaling behavior of dynamic properties, such as the zero-shear viscosity and the terminal relaxation time, can only be studied in the case of the fd virus. Note that although *F*-actin and fd filaments compared in this study have similar dimensions, they differ significantly with regard to polydispersity, which may strongly affect the network properties.

Finally, we compare the measured viscoelastic impedance spectra, $G'(f)$ and $G''(f)$, with the calculated values for the

complete frequency range by applying the recently published theory of Morse [13] (Fig. 7). This theory predicts the qualitative behavior for the complete spectra, but does not yet predict very well absolute values. Therefore, we treated the solvent viscosity, entanglement length, and tube diameter as free parameters to obtain the best fit between theoretical predictions and experimental data. Best fit was obtained by using a value of 0.63 μm for the entanglement length [implying a prefactor of 5.6 in the expression of $L_e \propto L_p(cLL_p^2)^{-2/5}$] and 76 nm for tube diameter. In Fig. 7, the G' and G'' values calculated according to Morse [13] for a 10 mg/ml fd solution are compared with the experimental data obtained by microrheometry and macrorheometry. Given the variance among the experimental data of the different techniques, their overall agreement with the theoretical curves is reasonably good with a few notable exceptions. For instance, the analysis by Morse predicts a broad plateau for storage modulus while the experiments show a rather narrow and slanted plateau, casting doubts about the applicability of the theoretical approach. We note that the narrowing of the plateau region has also been found in measurements of *F*-actin solutions with short average filament lengths down to 1.5 μm [50].

Our measurements of fd solutions reveal interesting features of semiflexible filaments at low frequencies. In the regime of viscous flow, one would expect solutions of semiflexible filaments to behave more like rigid rods, since the undulatory excitations are completely damped out. In this case, similar to the behavior of flexible chains, a scaling behavior of $G'(f) \propto f^2$ and $G''(f) \propto f^1$ is expected [44]. This behavior can be understood in terms of a simple Maxwell model equivalent to mechanical circuits [1]. Our measurements show that the frequency dependence for solutions of the semiflexible fd virus is remarkably weaker. We find $G'(f) \propto f^{0.9-1.2}$ and $G''(f) \propto f^{0.7-0.9}$ over one order of magnitude. The calculation by Morse predicts an exponent close to 1 for the scaling of $G'(f)$ at frequencies f just below the plateau. However, our data suggest that the transition to the rigid-rod-like behavior would only occur at much lower frequencies than probed by the current rheological measurements.

In summary, solutions of fd exhibit certain viscoelastic features that resemble those of solutions of *F*-actin of short mean filament length, including a narrow and slanted plateau region, a power law $G'_N \propto c_A^{7/5}$ for the plateau modulus, and a terminal relaxation time in the range of a few seconds. Using two independent species of semiflexible filaments to test the theoretical treatment ensures that the experimental results are not due to peculiar features of one particular system. Despite the remarkable similarities between the two types of semiflexible filaments, the short bacteriophage filaments show some distinct features, which are not observed for solutions of *F*-actin. The most notable feature is an anomalous frequency dependence of the viscoelastic storage and loss moduli below the plateau regime. In future studies, we will attempt to perform measurements in a broader frequency range, especially by extending measurements to higher-frequency regimes, for which interesting predictions have been made by several recent theoretical analyses [5,13,49].

ACKNOWLEDGMENTS

This work was supported by the Deutsche Forschungsgemeinschaft under Contract No. Sa. 246/22-4 (E.S.), and also by Brigham & Women's Hospital (Boston, MA) and Indiana University (J.X.T.). We are grateful to the late Irene Sprenger for her assistance in electron microscopy. We also thank Erwin Frey, Klaus Kroy, Paul Janmey, Fred MacKintosh, David Morse, and Jan Wilhelm for valuable suggestions and stimulating discussions. F.G.S. wishes to thank B.H. for fruitful collaboration over several years.

[1] J. Ferry, *Viscoelastic Properties of Polymers* (Wiley, New York, 1980).
[2] P. J. Flory, *Statistical Mechanics of Chain Molecules* (Interscience, New York, 1969).
[3] E. Frey, K. Kroy, and J. Wilhelm, in *The Wiley Polymer Networks Group Review Series*, edited by B. T. Stokke (Wiley, New York, 1999), Vol. 2.
[4] E. Frey, K. Kroy, and J. Wilhelm, in *Advances in Structural Biology*, edited by S. K. Malhotra and J. A. Tuszynski (Jai Press, London, 1998).
[5] F. Gittes and F. C. MacKintosh, Phys. Rev. E **58**, R1241 (1998).
[6] B. Hinner *et al.*, Phys. Rev. Lett. **81**, 2614 (1998).
[7] H. Isambert and A. C. Maggs, Europhys. Lett. **31**, 263 (1995).
[8] H. Isambert and A. C. Maggs, Macromolecules **29**, 1036 (1996).
[9] K. Kroy and E. Frey, Phys. Rev. Lett. **77**, 306 (1996).
[10] F. MacKintosh, J. Käs, and P. Janmey, Phys. Rev. Lett. **75**, 4425 (1995).
[11] A. C. Maggs, Phys. Rev. E **55**, 7396 (1997).
[12] A. C. Maggs, Phys. Rev. E **57**, 2091 (1998).
[13] D. Morse, Macromolecules **31**, 7044 (1998).
[14] D. Morse, Macromolecules **31**, 7030 (1998).
[15] D. Morse, Phys. Rev. E **58**, R1237 (1998).
[16] E. Sackmann, in *Modern Optics, Electronics and High Precision Techniques in Cell Biology*, edited by G. Isenberg (Springer-Verlag, Berlin, 1998), pp. 211–258.
[17] A. N. Semenov, J. Chem. Soc., Faraday Trans. 2 **82**, 317 (1986).
[18] J. Wilhelm and E. Frey (unpublished).
[19] P. A. Janmey *et al.*, J. Biol. Chem. **269**, 32 503 (1994).
[20] J. Xu, D. Wirtz, and T. D. Pollard, J. Biol. Chem. **273**, 9570 (1998).
[21] D. H. Wachsstock, W. H. Schwartz, and T. D. Pollard, Biophys. J. **65**, 205 (1993).
[22] P. A. Janmey *et al.*, Nature (London) **345**, 89 (1990).
[23] P. A. Janmey *et al.*, J. Biol. Chem. **261**, 8357 (1986).
[24] C. C. Cunningham *et al.*, Science **255**, 325 (1992).
[25] J. X. Tang *et al.*, Biophys. J. **76**, 2208 (1999).
[26] S. Bhattacharjee, M. J. Glucksmann, and L. Makowski, Biophys. J. **61**, 725 (1992).
[27] L. A. Day *et al.*, Annu. Rev. Biophys. Biophys. Chem. **17**, 509 (1988).
[28] E. Loh, Biopolymers **18**, 2569 (1979).

[29] E. Loh, E. Ralston, and V. N. Schumaker, Biopolymers **18**, 2549 (1979).
[30] T. Maeda and S. Fujime, Macromolecules **18**, 2430 (1985).
[31] L. Song *et al.*, Biopolymers **31**, 547 (1991).
[32] Z. Dogic and S. Fraden, Phys. Rev. Lett. **78**, 2417 (1997).
[33] H. Nakamura and K. Okano, Phys. Rev. Lett. **50**, 186 (1983).
[34] J. Tang and S. Fraden, Liq. Cryst. **19**, 459 (1995).
[35] A. P. Lyubartsev *et al.*, Phys. Rev. Lett. **81**, 5465 (1998).
[36] J. X. Tang *et al.*, Ber. Bunsenges. Phys. Chem. **100**, 796 (1996).
[37] J. Sambrook, E. F. Fritsch, and T. Maniatis, *Molecular Cloning: A Laboratory Manual* (Cold Spring Harbor Laboratory Press, Cold Spring Harbor, NY, 1989).
[38] F. G. Schmidt, F. Ziemann, and E. Sackmann, Eur. Biophys. J. **24**, 348 (1996).
[39] F. G. Schmidt, B. Hinner, and E. Sackmann, Phys. Rev. E **61**, 5646 (2000).
[40] F. Ziemann, J. Rädler, and E. Sackmann, Biophys. J. **66**, 2210 (1994).
[41] O. Müller *et al.*, Macromolecules **24**, 3111 (1991).
[42] M. Tempel, G. Isenberg, and E. Sackmann, Phys. Rev. E **54**, 1802 (1996).
[43] A. Palmer *et al.*, Biophys. J. **76**, 1063 (1999).
[44] M. Doi and S. F. Edwards, *The Theory of Polymer Dynamics* (Oxford University Press, Oxford, 1992).
[45] C. F. Schmidt *et al.*, Macromolecules **22**, 3638 (1989).
[46] T. Odijk, Macromolecules **16**, 1340 (1983).
[47] L. Onsager, Ann. N. Y. Acad. Sci. **51**, 627 (1949).
[48] K. Kroy (private communication).
[49] R. Everaers *et al.*, Phys. Rev. Lett. **82**, 3717 (1999).
[50] J. X. Tang (unpublished data).
[51] B. Hinner (unpublished data).